Neural Computing and Applications (2021) 33:821–835
https://doi.org/10.1007/s00521-020-05249-z

S.I. : ATCI 2020

Prediction of energy photovoltaic power generation based on artificial intelligence algorithm

Shuhua Zhang[1,2] · Jinsong Wang[3] · Haibo Liu[4] · Jie Tong[2] · Zheng Sun[5]

Received: 28 April 2020 / Accepted: 25 July 2020 / Published online: 5 August 2020

Abstract
The key to the coordination of photovoltaic power generation and conventional energy power load lies in the accurate prediction of photovoltaic power generation. At present, prediction models have problems with accuracy and system operation stability. Based on the neural network algorithm, this research carries the prediction of energy photovoltaic power generation and establishes a BP neural network prediction model and a wavelet neural network prediction model. Moreover, this research studies the influence of various factors on the prediction t of photovoltaic power generation, and analyzes the relationship between the various factors. In addition, in this study, a comparative test is constructed to analyze the model performance, and a statistical graph is drawn to take a visual comparison of performance. The research shows that the model proposed in this paper has certain effects and has certain advantages in the prediction of photovoltaic power generation.

Keywords Artificial intelligence algorithm · Energy · Neural network · Power generation · Prediction model

1 Introduction

Energy is an important material foundation for the survival and development of human society. In the course of the development of human society, every major turning point in human civilization is accompanied by the improvement and replacement of energy utilization methods. The progress of energy development and utilization has an important impact on the development of the world economy, technology and human society. With the continuous acceleration of socio-economic development, human demand for energy continues to increase. According to the survey, based on existing reserves and extraction rates, traditional energy sources such as coal, oil and natural gas can only be maintained for more than a 100 years. In recent years, the increase of pollutants emitted by traditional energy combustion has brought serious air pollution to most of our country. In particular, the frequent occurrence of haze in recent years has caused a serious impact on the health and life of the people in China. Accelerating the development and utilization of renewable energy and replacing traditional fossil energy with new green renewable energy are long-term strategies to alleviate the energy crisis and improve environmental problems [1]. Renewable energy refers to energy that can be continuously regenerated in the natural world and can be continuously used, which has the advantages of inexhaustible. At present, the main new green energy sources include solar energy, wind energy, biomass energy, tidal energy, geothermal energy and hydropower, etc. Due to the short development time of new energy utilization, many new energy utilization technologies are still immature. In particular, the shortcomings in the development and

✉ Shuhua Zhang
1182101048@ncepu.edu.cn

1 School of Electrical and Electronic Engineering, North China Electric Power University, Beijing 102206, China

2 China Electric Power Research Institute Co., Ltd., Beijing 100192, China

3 Department of Electrical, Computer, and System Engineering, Case Western Reserve University, Cleveland, OH 44106, USA

4 Department of Science and Technology, State Grid Inner Mongolia Eastern Power Co., Ltd, Hohho 010010, China

5 Department of Electronic and Communication Engineering, North China Electric Power University, Baoding 071003, China

utilization technology make the cost of new energy development and utilization higher than traditional energy. At present, there is no new energy that can replace the dominant role of fossil energy in the global use. Moreover, power generation strategies are different between different energy systems, and different energy utilization methods will also bring inconvenience to the management and operation of the power grid. Therefore, efficient coordination between different energy systems requires optimization of control strategies between power grids. It can be said that overall planning for the utilization of different energy sources and optimization of grid connection strategies are important research directions for comprehensive utilization of new energy sources [2].

In recent years, in order to complete the sustainable development strategy of energy and environment, governments around the world have taken photovoltaic power research as a key project for new energy research and development. However, because the photovoltaic system's power generation is not only seriously affected by the randomness of the external weather, but also by the internal characteristics of the photovoltaic modules, the output power of the photovoltaic power generation system has shortcomings such as intermittent and large fluctuations. In order to make the above-mentioned shortcomings of the photovoltaic system to minimize the impact on the grid after grid connection, people began to pay attention to the photovoltaic power generation prediction technology [3]. There are many factors that affect the output of photovoltaic power generation systems. The external meteorological factors are solar radiation intensity, ambient temperature and relative humidity. The elements of the internal photovoltaic module are the type of the battery panel, the area and temperature of the battery panel, and the installation angle of the battery panel. All internal and external factors are coupled together to form a multivariable, strongly coupled, severely nonlinear relationship that affects the output power of photovoltaic cells. As mentioned above, if every element that affects the output power of photovoltaic cells is listed as the input of the prediction model, the complexity of the model will inevitably increase, and more input variables will affect the calculation speed of the photovoltaic power generation prediction model, resulting in a decrease in the timeliness of the prediction and the failure of the model prediction. If only the solar radiation intensity, shadow occlusion, and panel temperature are considered as the main influencing factors, the use of simplified model prediction will definitely affect the prediction accuracy, which will lead to a decline in the availability of the prediction [4]. For this reason, on the basis of fully grasping the internal and external factors that affect the nonlinear coupling of photovoltaic power generation, the establishment of a reasonable forecast of power generation under all operating conditions will help improve the accuracy and speed of forecasting, control the impact of large-scale photovoltaic access on existing power grids, realize the coordination of photovoltaic power generation and conventional energy power loads, and obtain greater economic and social benefits.

2 Related work

Nowadays, more and more solar energy is used by people, and the trend of photovoltaic grid connection is also increasing. At the 2015 International Solar Technology Expo in Munich, Germany, the PV Market Alliance released the "PV Market Report" for the first time. The report estimates that the installed photovoltaic capacity worldwide will reach 50 GW by the end of 2015 and will reach about 70 GW by 2020. Solar cell power generation has become one of the fastest growing energy supply methods in the world [5]. Following the Fukushima nuclear pollution accident in 2011, the development and utilization of solar energy was increased. The Japanese government has invested a lot of funds in the construction of large-scale photovoltaic power stations. The government has introduced relevant policies to stabilize electricity prices and provide substantial preferential policies for photovoltaic power generation. This has led to the rapid and balanced development of the Japanese photovoltaic industry in recent years. According to the "Low Carbon Society Action Plan" proposed by Japan, the total installed capacity of Japan is expected to reach 14GW by 2020 [6]. Based on the development experience of photovoltaic power generation applications in European Union countries, the United States, Japan and other countries, it is not difficult to find that the development of the photovoltaic industry in a country mainly depends on the leading role of government departments. Moreover, the main driving force for its rapid development is the various preferential and subsidy policies issued by the government. The means of promotion is mainly to encourage and promote the development of the solar energy industry through the government's high-priced purchase of electricity generated by solar energy. When it reaches a sufficiently large economic scale in the future, it can be adjusted by the market and gradually reduce the cost of solar cell power generation to make solar power generation widely used.

Since the discovery of solar energy for power generation, research on solar energy utilization technology has never stopped. As the situation of the energy crisis and environmental pollution becomes more and more serious, the application of solar energy has received unprecedented attention. Among them, the integration of photovoltaics

into large power grids has become a trend of using solar energy. Because photovoltaic power generation has certain characteristics of volatility, indirectness, and uncontrollability, it will easily affect grid dispatching, distribution, and other work after grid connection, and may even damage the grid or cause accidents. In order to avoid such safety accidents, we can predict the power generation of the photovoltaic system before incorporating it into the large power grid, so as to better manage the power grid reasonably. In recent years, photovoltaic power generation forecasting technology has become a research hotspot both at home and abroad. According to a large amount of literature, it is found that the existing photovoltaic prediction methods are roughly divided into mathematical statistics, artificial intelligence prediction methods, and emerging prediction methods [7]. Mathematical statistics method is mainly a method of statistical analysis and speculation directly through a large number of historical data of power stations. The forecast time is within 0–1 h, and its advantage is that there is no requirement for the location of photovoltaic power stations and power conversion parameters [8]. The disadvantages are that the prediction time scale is short, the data dimension is large, and the redundancy is high. Mathematical statistics method generally includes gray theory prediction method, multiple linear regression prediction method, time-series prediction method, and so on. For example: the literature [9] introduced the gray prediction model GM (1,1), and improved it based on the shortcomings of the model, and then established an improved gray prediction model. At the same time, training and verification were performed using data from Jiangsu Province's power generation from 2000 to 2009. The results show that the gray prediction model can predict the amount of photovoltaic power generation, but the improved prediction model not only enhances the smoothness of data fitting, but also improves the accuracy of prediction results. The literature [10] established a multivariate linear regression grid-connected photovoltaic prediction model, which takes into account factors such as light intensity, ambient temperature, actual panel temperature, and wind conditions. The results of the F-test method show that the model can fit the forecast data well, and it can also improve the accuracy of the forecast results under different weather types. Artificial intelligence prediction methods have been developed with the development of computer science. At present, neural network prediction methods, support vector machine prediction methods, and improved prediction methods based on these two prediction methods are commonly used. For example, the literature [11, 12] used historical power generation data and meteorological factor data of power stations to train BP neural network models and use them to predict photovoltaic power generation. The literature [13] has carried out in-depth research on the prediction of support vector machines in the field of power systems. In the literature [14], Ran Li and Guangmin Li introduced the principle and process of establishing a support vector machine mathematical model in detail, and trained and predicted the model with historical photovoltaic power generation data in Baoding, Hebei. The article concludes that support vector machines are feasible as a method for generating power generation prediction, but the disadvantage is that the prediction accuracy is not very high. Improved algorithms based on neural network algorithms include the neural network prediction method based on Newton's wavelet [15], the neural network prediction method based on genetic algorithm [16], and the Markov chain prediction methods based on BP neural networks [17], and BP neural network prediction methods based on particle swarm optimization [18]. The least squares support vector machine prediction model based on robust learning [19] and the similarity-based least squares support vector machine prediction model [20] are based on the support vector machine prediction model to add some improved algorithms to improve the prediction accuracy of the prediction model. From the current overall situation, the application of artificial intelligence prediction methods in the actual large-scale photovoltaic power plant prediction system is still very small. The main reason is that its algorithm is too theoretical. If it is to be widely applied to engineering practice, it needs a lot of research and analysis with the help of computer simulation software, so that it can be used reasonably and effectively in various occasions in the future. The emerging photovoltaic power generation forecasting method mainly uses astronomical radiation obtained from satellite cloud image data as the input of the prediction model, and then uses the actual solar radiation received by the photovoltaic panel as an output to establish a prediction model to predict the photovoltaic power generation indirectly, such as, the Hottel radiation prediction model and Liu-Jordan radiation model in [21]. However, this method is very difficult to implement, and research on this aspect at home and abroad is still in its infancy.

3 Forecasting model of photovoltaic power generation based on fuzzy neural network

3.1 Model feasibility analysis

Before the experiment, the feasibility analysis of the model in this paper is helpful to understand whether the model algorithm is suitable when facing the photovoltaic system and provides certain guidance for the subsequent algorithm implementation. After the feasibility analysis, if the analysis results show that the algorithm is not suitable for the

photovoltaic system, the existing algorithm needs to be replaced. However, if the analysis results show that the algorithm is suitable for photovoltaic systems, it will be more effective in the subsequent model building process. The daily power generation of photovoltaic systems is shown in Fig. 1.

As shown in Fig. 1, the daily power generation of photovoltaic systems presents a very irregular random characteristic. The reason is that the performance of solar cells is greatly affected by environmental factors. Therefore, in order to obtain more accurate forecast results, in this paper, the historical power generation data and actual meteorological data at the corresponding time are used in the photovoltaic system, and the fuzzy neural network method combining fuzzy theory and neural network is used to realize the short-term forecast function of photovoltaic system power generation. It can be clearly seen from Fig. 1 that the distribution of power generation in the chronological order is extremely irregular, while the daily power generation of the same weather characteristics has extremely similar characteristics. The use of fuzzy theory to improve the prediction model can very well reduce the impact of sharply changing weather factors on power generation, and play a role in optimizing and improving the prediction model. All in all, the fuzzy neural network method using a combination of fuzzy theory and neural network has a certain desirability for short-term prediction of the daily power generation of photovoltaic systems.

The fuzzy neural network model can handle complex systems with little information well, does not require a large amount of data for modeling, and is very simple to implement, so it is already a relatively complete theoretical system, and the model has been applied to many field.

3.2 Model overview

The data provided in this article mainly includes irradiance, humidity, temperature, wind speed, and evaporation. The relationship between these meteorological factors and the amount of photovoltaic power generation has also been explained above. Therefore, we can use this data to form the basic input data space of the model. The influence of weather factors on the output power of photovoltaic systems is shown in Fig. 2.

Figure 2 shows that although the daily power of photovoltaic systems is different and random, when the weather types are the same, although the output curves of the photovoltaic systems are different, the shapes are very similar, and the trends are basically the same. However, when the weather types are inconsistent, the system output curves under different weather conditions are quite different and their shapes are basically different. It can be seen that if the same network is used to fit all the weather data, the network will take a long time to learn and require a large number of learning samples. Moreover, such complicated data and models will make the prediction accuracy of the model lower. Therefore, in this paper, according to the classification of weather types, different prediction models are established to correspond to different weather types. When a complex network is split into three different weather types and fitted separately, the learning time of the model is reduced and the prediction accuracy of the model is improved. Moreover, the data of meteorological factors such as irradiance, humidity, temperature, wind speed, and evaporation that affect photovoltaic systems are used as inputs to the prediction model.

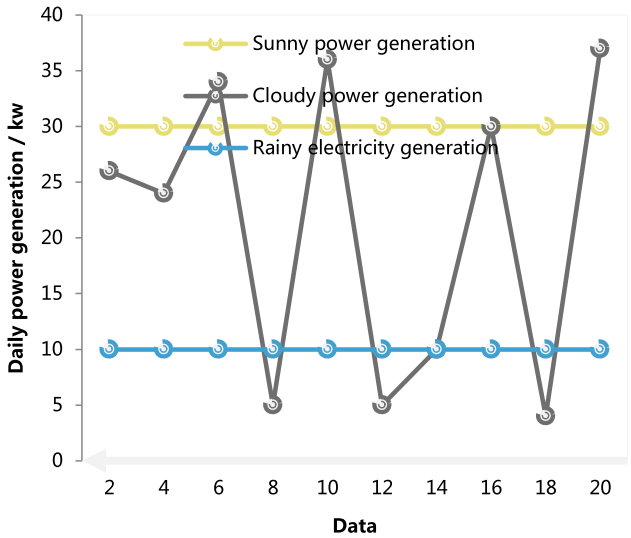

Fig. 1 The graph of the change of the daily power generation of photovoltaic systems

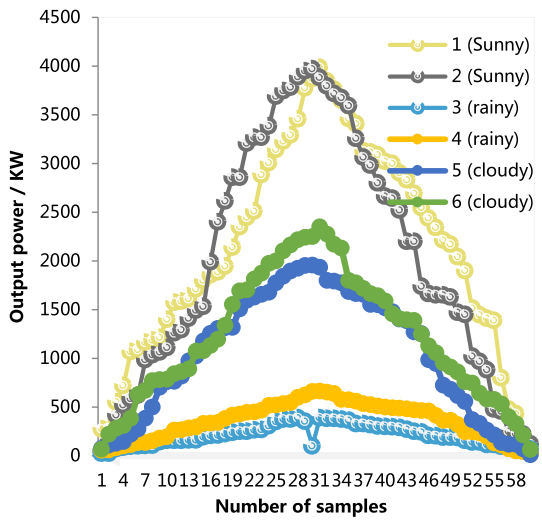

Fig. 2 The influence of weather factors on the output power of photovoltaic systems

3.3 Classify samples by weather type

In the weather system, the common types are sunny, cloudy, overcast, rain, shower, thunder shower, sleet, light rain, moderate rain, heavy rain, light snow, moderate snow, heavy snow, blizzard, fog, freezing rain, sandstorm, haze, etc. As can be seen from the above, under different weather conditions, the photovoltaic system's power generation curve is very different. After sorting and analyzing the historical power generation data and corresponding weather data of the photovoltaic system, the main weather types in this paper are divided into three types: sunny, cloudy, and rainy. When different weather types are classified, the combination types such as cloudy to sunny and sunny to cloudy are classified as sunny, the combination types such as cloudy to cloudy are classified as cloudy, and rain and snow are all classified as rainy. The historical power generation data corresponding to the time is also divided by weather type.

This article classifies data by weather type, and builds prediction models with three models: sunny, cloudy, and rainy. The sample data is also classified according to this type and the corresponding data is assigned to the corresponding sub-model for training. The overall framework of the model is shown in Fig. 3.

4 Sub-model neural network algorithm

Based on neural network theory, its learning algorithm is mainly composed of two parts: one is the structure determination part of the network; the second is the network center determination and weight learning correction part. The center is generally determined by a random method, and the weight learning correction method usually uses K-means clustering method, center supervised selection method, regularized strict interpolation method, orthogonal least square method, and the like.

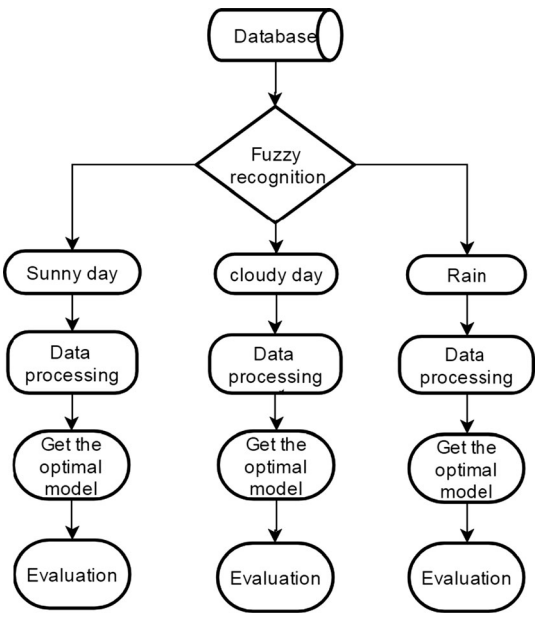

Fig. 3 Overall framework of the model

4.1 Determination of network structure

Each predictor model is a fuzzy neural network corresponding to the weather type. After training the network with different weather type data, the prediction accuracy of the corresponding weather type data is higher than that of neural networks when the weather type is not distinguished. After the sample is divided into three categories, a sub-model is set for each category. The input of the sub-model consists of meteorological factors in this type of weather: irradiance, temperature, humidity, wind speed, and evaporation. The output is the corresponding power generation data during the training process and is the predicted value of the power generation during prediction. The fuzzy neural network generally has a four-layer structure, an input layer, a fuzzification layer, a rule calculation layer, and an output layer. The sub-model network structure is shown in Fig. 4.

4.2 Network center determination and weight learning correction

At present, there are many learning algorithms that can be used to determine cluster centers in neural network algorithms. The most important is the random selection method (that is, the direct calculation method). This method is to randomly select or use all the inputs in the sample as the center of the basis function of the network, and the center position and number are fixed, and then the width (i.e., the

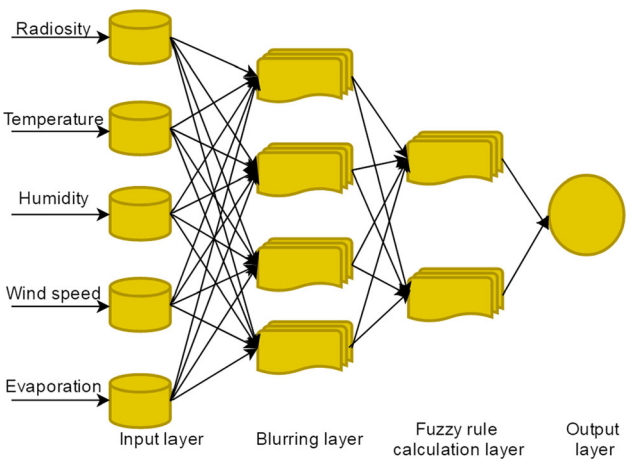

Fig. 4 Structure of the sub-model network

variance) of the network can be determined. When the center and width are known, the output layer matrix is determined, and the connection weights of the neural network can be determined by solving the linear equations.

In the process of correcting network weights, gradient descent can be used to correct and learn network errors. After determining the center c_i of the network, due to the linear mapping relationship between the hidden layer and the output layer, the weights between the hidden layer and the output layer can be determined by the least square method and the least recursion method.

1. Least squares learning weights w_i. We assume the output vector is $w = (w_1, w_2, \ldots, w_m)^T$. It can be directly calculated using the least square method (LMS). The specific algorithm steps are as follows: If the input is set to $x_j, j = 1, 2, 3, \ldots,$, the output of the i-th hidden layer node is h_{ji}, and the expression of h_{ji} is:

$$h_{ji} = \phi(\|x_i - c_i(k)\|) \tag{1}$$

In the formula, a Gaussian function $\phi_i(\cdot)$ is used as the activation function of a hidden layer node. Therefore, the hidden layer output matrix of the network can be defined as $\hat{H}$, and the expression is $\hat{H}$:

$$\hat{H} = \left[h_{ji}\right], \hat{H} \in R^{N*N} \tag{2}$$

Then, $\hat{H} \in R^{L*M}$. If the current weight of the RBF network is $w = [w_1, w_2, \ldots, w_m]^T$, then for all samples, the network output vector is $\hat{y}$, and the expression of $\hat{y}$ is as follows:

$$\hat{y} = \hat{H}w \tag{3}$$

In order to obtain the output weight of the network, the approximation error of the network is defined as $\varepsilon = \|y - \hat{y}\|$. If the teacher signal $y = [y_1, y_2, \ldots, y_N]^T$ of the network is given and $\hat{H}$ is determined, the output weight w of the network can be obtained by using the minimum value of the approximation error ε. The expression of ε is as follows:

$$\varepsilon = \|y - \hat{y}\| = \left\|y - \hat{H}w\right\| \tag{4}$$

Generally, w can be obtained by the least square method, and the expression of w is as follows:

$$w = \hat{H} * Y \tag{5}$$

In the formula, $\hat{H}^*$ is the pseudo-inverse of $\hat{H}$, and the expression of $\hat{H}^*$ is as follows:

$$\hat{H}^* = \left(\hat{H}^T\hat{H}\right)^{-1}\hat{H}^T \tag{6}$$

2. We assume that the output vector is $w = [w_1, w_2, \ldots, w_m]^T$. It is trained using the gradient method, a supervised learning method. The specific steps of the algorithm are as follows:

(a) In the input vector, a set of initial center values are selected and recorded as C_k.

(b) The variance value σ is calculated. The expression of σ is as follows:

$$\sigma = d_{\max}/K \tag{7}$$

In the formula, $d_{\max}$ is the maximum distance between the centers, and K is the number of center values C_k.

(c). By the input $x(n)$, $\hat{y}_i(n)$ is calculated. The expression of $\hat{y}_i(n)$ is as follows:

$$\hat{y}_i(n) = \sum_{k=1}^{M} W_K \phi[x(n), C_k, \sigma_k] \tag{8}$$

(d) Network parameters $W(n), C(n), \sigma(n)$ are update. After the update, the expression for $W(n+1), C_K(n+1), \sigma_K(n+1)$ is as follows:

$$W(n+1) = W(n) + \mu_W e(n)\phi(n) \tag{9}$$

$$\begin{aligned} &C_K(n+1) = C_K(n) + \mu_C \frac{e(n)W_K(n)}{\sigma_K^2(n)} \\ &\phi[x(n), C_K(n), \sigma_K(n)][x(n) - C_K(n)] \end{aligned} \tag{10}$$

$$\begin{aligned} &\sigma_K(n+1) = \sigma_K(n) + \mu_\sigma \frac{e(n)W_K(n)}{\sigma_K^2(n)} \\ &\phi[x(n), C_K(n), \sigma_K][x(n) - C_K(n)] \end{aligned} \tag{11}$$

In the formula,

$$\begin{aligned} &\phi(n) = \\ &\{\phi[x(n), C_1(n), \sigma_1], \phi[x(n), C_2(n), \sigma_2], \ldots, \\ &\phi[x(n), C_N(n), \sigma_N]\} \end{aligned} \tag{12}$$

$$e(n) = \hat{y}_i(n) - y_d(n) \tag{13}$$

In formulas (9)–(13): $y_d(n)$ is the expected output of the network; μ_N, μ_C and μ_σ are the learning step size of 3 parameters.

(e) Whether the network is converged is judged. If the network converges, the calculation stops. However, if the network does not converge, the algorithm jumps to step (4) to continue the calculation until the network converges.

3. To simplify the problem, a recursive least squares (RLS) method is used to analyze the single output case. Due to the characteristics of the algorithm, the convergence of the LMS is determined by the eigenvalue distribution of the matrix R. If the eigenvalue distribution is large, the algorithm's convergence speed is slower. However, if the eigenvalue distribution is small, the algorithm will converge faster. The problem of unstable convergence speed can be better avoided by using RLS. When using RLS, its main optimization goal is to obtain the smallest weight-squared error, that is, the minimum value of the performance function $\xi = \lambda^{n-k}\left|e(n)^2\right|$. In the formula, λ is the forgetting factor. Its value is less than 1 but close to 1. Its function is mainly to weight historical data, so that the algorithm can forget historical data far enough (that is, beyond the amount of memory). The memory of the algorithm is $1/1-\lambda$. The algorithm flow is as follows:

When the initial conditions are given:

$$w(0) = x(0) = 0, C(0) = \delta^{-1}I$$

δ is a positive real number and the value is small and I is the identity matrix. The iterative algorithm is used, $n = 1, 2, 3, \ldots,$

(a) The center distance $d(n)$ and the input $x(n)$ are obtained;

(b) The gain vector $g(n)$ is updated, and the updated expression is as follows:

$$g(n) = (C(n-1)x(n))/(\lambda + \mu(n)) \tag{14}$$

In the formula, the expression of $\mu(n)$ is as follows:

$$\mu(n) = x^H(n)C(n-1)x(n) \tag{15}$$

(c) The weight vector $w(n)$ is updated. The updated expression is as follows: Update the weight vector. The updated expression is as follows:

$$w(n) = w(n-1) + g(n)\left[d(n) - x^H(n)w(n-1)\right]^* \tag{16}$$

(d) The inverse matrix $C(n)$ is updated. The updated expression is as follows:

$$C(n) = \lambda^{-1}\left[C(n-1) - g(n)x^H(n)C(n-1)\right] \tag{17}$$

(e) The algorithm returns (a).

Compared with the least squares method (LMS), the recursive least squares method (RLS) does not need to know the eigenvalue distribution of the matrix R to determine the convergence of the algorithm, and the convergence speed is faster. However, the disadvantage is that the complexity of the calculation process is high, and it has a large amount of calculation.

In practical applications, training samples usually contain noise in the context of pattern recognition or nonlinear regression. Moreover, when the hidden layer and the input sample are the same size, it may lead to a waste of computing resources. If the training samples have a large scale, the waste of resources during processing is particularly serious. Therefore, we need to continuously modify the weights of the network so that the network can better process the samples.

5 Predictive model

5.1 Fuzzy model

When using a fuzzy model, the model needs to be adaptive, capable of being automatically updated, and the membership function of the fuzzy set must be continuously modified to obtain a more suitable model. In this paper, if–then rules can be used to define the model. If the rule is R^i, then the expression of R^i is:

$$\begin{aligned} &\text{if } \ x_1 \text{ is } A_1^i, x_2 \text{ is } A_2^i, \ldots, x_k \text{ is } A_k^i, \text{then} \\ &\quad y_i = p_0^i + p_1^i x_1 + \cdots + p_k^i x_k \end{aligned} \tag{18}$$

In the formula, A_j^i is the fuzzy set of the fuzzy system, y_i is the parameter of the fuzzy system, and $p_j^i (j = 1, 2, \ldots, k)$ is the output generated by the fuzzy system. In this model, if is fuzzy as input and then is certain as output. The fuzzy rule reasoning is that the output is a linear combination of inputs.

When using fuzzy rules, we must first determine the membership of the input variables. If the input is $x = [x_1, x_2, \ldots, x_k]$, the expression of membership μA_j^i is as follows:

$$\mu A_j^i = \exp\left(\frac{-\left(x_j - c_j^i\right)^2}{b_j^i}\right) \quad j = 1, 2, \ldots, k; \;\; i = 1, 2, \ldots, n \tag{19}$$

In the formula, c_j^i is the center of the membership function, b_j^i is the width of the membership function, k is the number of output parameters, and n is the number of fuzzy subsets. The degree of membership is calculated using a multiplication operator. The expression of the multiplication operator w_i is as follows:

$$w_i = \mu A_j^1(x_1) * \mu A_j^2(x_2) * \cdots * \mu A_j^k(x_k), \quad i = 1, 2, \ldots, n \tag{20}$$

The expression of the output value y_i of the fuzzy model is as follows:

$$y_i = \frac{\sum_{i=1}^{n}\left(p_0^i + p_1^i x_1 + \cdots + p_k^i x_k\right) * w^i}{\sum_{i=1}^{n} w^i} \tag{21}$$

When using a fuzzy neural network, its structure must first be determined. The input layer is determined by the input vector, and its number is generally consistent with the dimensionality of the input data. The function of the fuzzification layer is to calculate the input data using the membership function formula (19) to obtain the membership value. The rule calculation layer uses the fuzzy operator w_i to calculate the membership value. The fuzzy operator used in this paper is the continuous multiplication operator. The output layer uses a formula to calculate the output value of the entire fuzzy neural network. The specific steps are as follows:

1. The error e is calculated. The expression of e is as follows:

$$e = \frac{1}{2}(y_d - y_c)^2 \tag{22}$$

In the formula, y_d is the expected output of the network, and y_c is the actual output of the network.

2. The coefficient p_j^i is corrected, and the expression of p_j^i after correction is as follows:

$$p_j^i(k) = p_j^i(k-1) - \alpha\frac{\partial e}{\partial p_j^i} \tag{23}$$

$$\frac{\partial e}{\partial p_j^i} = \frac{(y_d - y_c)w^i}{\sum_{i=1}^{m} w^i} \tag{24}$$

In the formula, p_j^i is the neural network coefficient, α is the network learning rate, x_j is the input parameter, and w^i is the continuous product of membership.

3. Parameter correction. The expression of c_j^i and b_j^i after correction is as follows:

$$c_j^i(k) = c_j^i(k-1) - \beta\frac{\partial e}{\partial c_j^i} \tag{25}$$

$$b_j^i(k) = b_j^i(k-1) - \beta\frac{\partial e}{\partial b_j^i} \tag{26}$$

In the formula, c_j^i is the center of the membership function, and b_j^i is the width of the membership function.

5.2 Training of fuzzy neural networks

The prediction model based on fuzzy neural network is shown in the previous section. The input of training data is five parameters: irradiance, temperature, humidity, wind speed, and evaporation. It can be determined that the number of input nodes of the network is 5. The output is the power generation amount, and the output node of the network is determined to be 1. The structure of the network is 5-12-1. The center and width of the fuzzy membership function are randomly obtained by the random selection method.

The fuzzy neural network is initialized, and the training data is normalized. The network was trained separately using data from three weather conditions. The results of model training under different weather conditions are shown in Fig. 5.

Figure 5 shows that the model fits the training data well under three different weather types.

6 Experimental research

The experimental device is mainly composed of photovoltaic cells, digital temperature and humidity meter, light intensity detector, light intensity tester, anemometer, non-contact infrared thermometer, KEITHLEY2400-72-1, Labview software and PC. The experimental device schematic is shown in Fig. 6. Polysilicon battery pack rated power: 2 W; maximum operating voltage: 6 V; maximum open-circuit voltage: 7.1 V; maximum short-circuit current: 330 mA; size: 135 mm * 125 mm; maximum open-circuit voltage: 18 V; maximum output power: 2.7 W; size: 200 mm * 150 mm. The atmospheric temperature and relative humidity meters are AR807 thermometers and

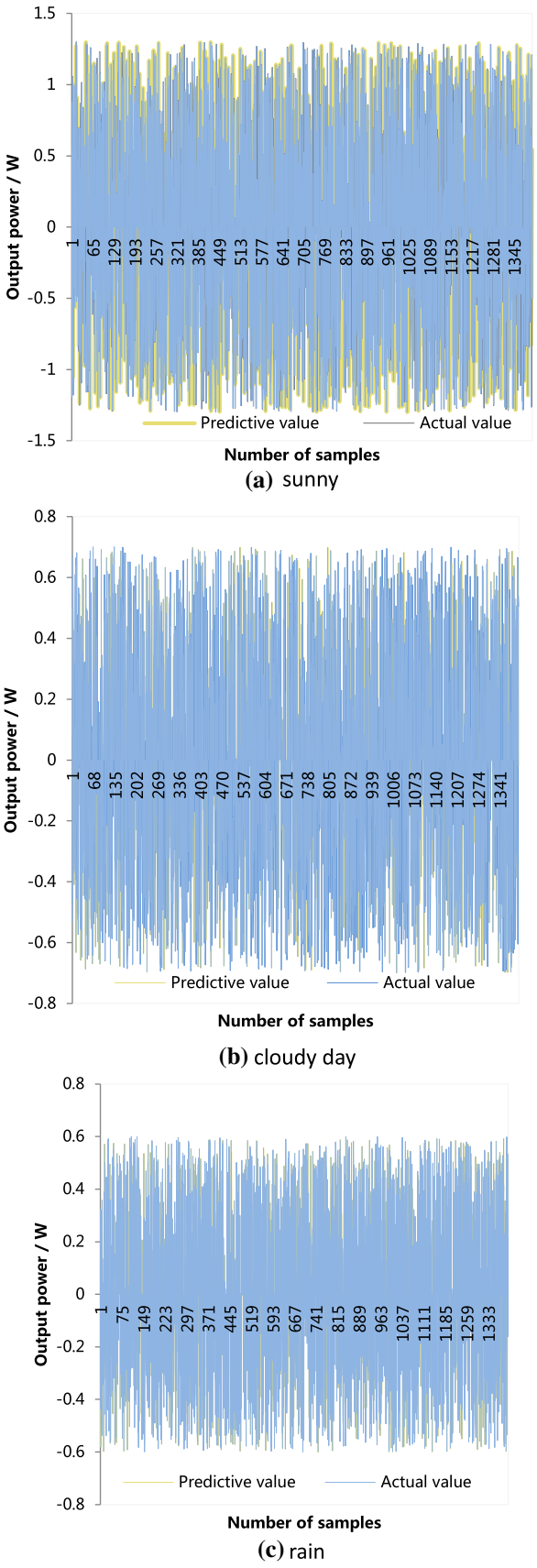

Fig. 5 Model training results under different weather conditions

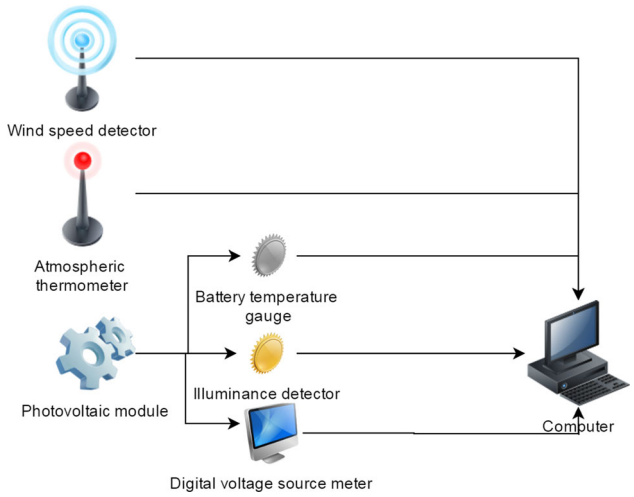

Fig. 6 Schematic diagram of the experimental device

hygrometers, the battery temperature meters are AR320 non-contact infrared thermometers, and the wind speed detector is an anemometer model AR816. In addition, the light irradiance detector is a type HT-855 light meter, and the light source uses natural light.

Figure 7 is a comparison result of the predicted value of the BP neural network and the measured value of the polycrystalline silicon under various input conditions. First, it can be seen that the prediction results of the BP neural network and the measured values generally agree well under various input conditions, and the model can better reflect the daily variation law of the maximum output power of photovoltaic power generation. Secondly, it can be seen that the prediction and measurement values under the conditions of light irradiance, battery temperature, and

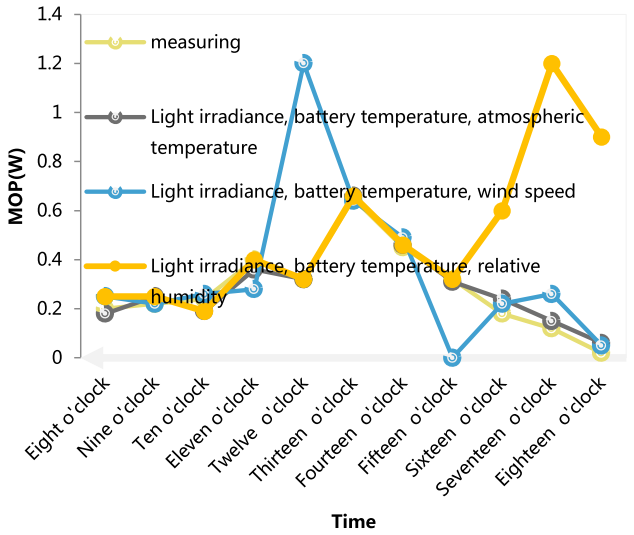

Fig. 7 Comparison of BP neural network prediction results and measured values for polycrystalline silicon under various input conditions

atmospheric temperature input agree best (the black line in the figure). The reason is that the light irradiance, battery temperature and atmospheric temperature have the most direct physical relationship with the output power of the battery, and have the strongest correlation. Then, it can be seen that there is a large error between the predicted and measured values under the conditions of light irradiance, battery temperature and wind speed input around noon (that is, between 11:00 and 14:00) (red line in the figure). The reason is that at this time the ambient temperature is high, the air convection is obvious, the wind speed changes drastically, and the output power of the battery fluctuates greatly, which causes the correlation between the output power and the wind speed to weaken and further to produce a large error in prediction. Finally, it can be seen that after 17 o'clock, there is a clear error between the predicted and measured values under the conditions of light irradiance, battery temperature and relative humidity input. The reason is that because the predicted time point is close to the western setting of the sun, the relative humidity in the area rises significantly, and the nonlinear correlation between the relative humidity and the battery output power is weakened, which causes the prediction to fail when the light irradiance and battery temperature are low.

Table 1 and Fig. 8 are the sum of squared error, mean square error, number of iterations, and training time of the network training under various input conditions. Table 1 shows that the sum of squared error and mean square error of the network training under the input conditions of light irradiance, battery temperature and atmospheric temperature is the smallest, and the network iteration and training time is the fastest. It shows that the polycrystalline silicon battery power generation has the closest correlation with the atmospheric temperature, so the prediction error is small and the running speed is fast. In addition, it can be seen that relative to the prediction under the input conditions of light irradiance, battery temperature, and relative humidity, the network training with the light irradiance, battery temperature, and wind speed as input conditions has

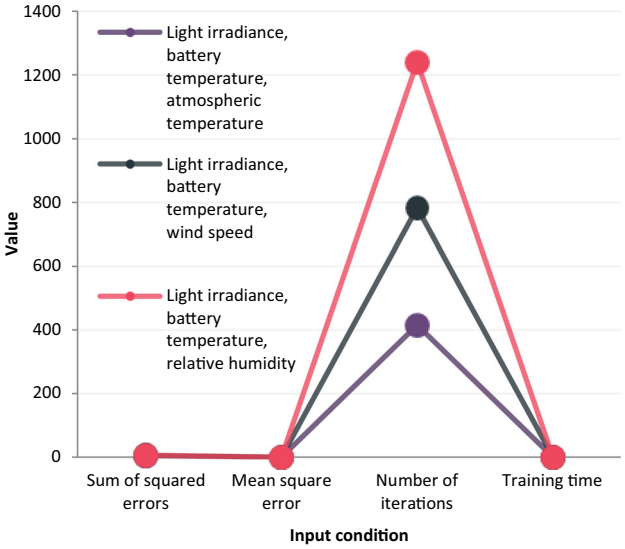

Fig. 8 Statistic diagram of sum of squared error, mean square error, number of iterations, and training time of network of polycrystalline silicon under various input conditions

large errors, but it runs fast. This shows that when there is a weak correlation between the amount of input and the amount of prediction, there is an inverse relationship between training error and speed.

Figure 9 is a comparison result of the predicted value of the BP neural network and the measured value of the amorphous silicon under various input conditions. First, it can be seen that the prediction results of the BP neural network and the measured values generally agree well under various input conditions, and the model can better reflect the daily variation law of the maximum output power of photovoltaic power generation. Secondly, it can be seen that around noon (that is, between 11:00 and 14:00), the errors between the predicted and measured values under the conditions of light irradiance, battery temperature, and wind speed input are large. The reason is that at this time the ambient temperature is high, the air convection is obvious, the wind speed changes drastically,

Table 1 Statistic table of sum of squared error, mean square error, number of iterations, and training time of network of polycrystalline silicon under various input conditions

	Light irradiance, battery temperature, atmospheric temperature	Light irradiance, battery temperature, wind speed	Light irradiance, battery temperature, relative humidity
Sum of squared errors	4.717912	6.324216	5.929811
Mean square error	0.017271	0.023129	0.021715
Number of iterations	415.11	782.75	1240.28
Training time	0:00:09	0:00:17	0:00:27

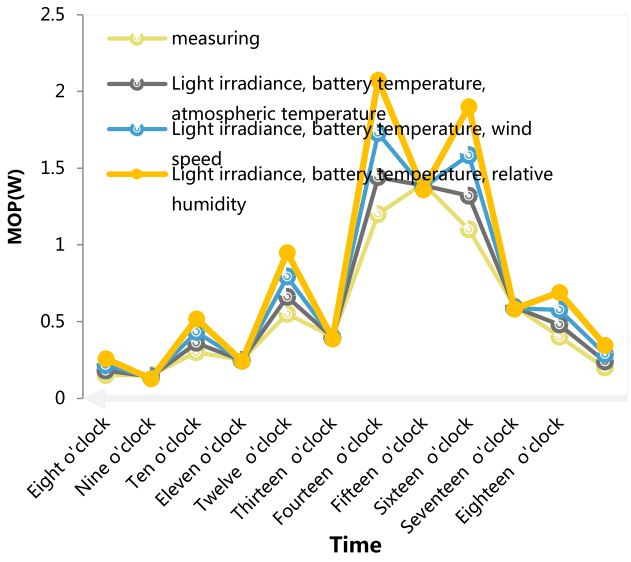

Fig. 9 Comparison of BP neural network prediction results and measured values of amorphous silicon under various input conditions

and the output power of the battery fluctuates greatly, which causes the correlation between the output power and the wind speed to weaken and further causes a large error in prediction. Finally, by comparing Figs. 8 and 10, it can be seen that under the premise of the sun setting and the relative humidity increasing, the predicted value of the amorphous silicon battery has not caused the error to fail. This shows that the relative humidity is weakly related to the nonlinearity of the amorphous silicon battery. However, by comparing Fig. 8, it is not obvious that the influence of atmospheric temperature on the amorphous silicon battery is stronger than the relative humidity. Therefore,

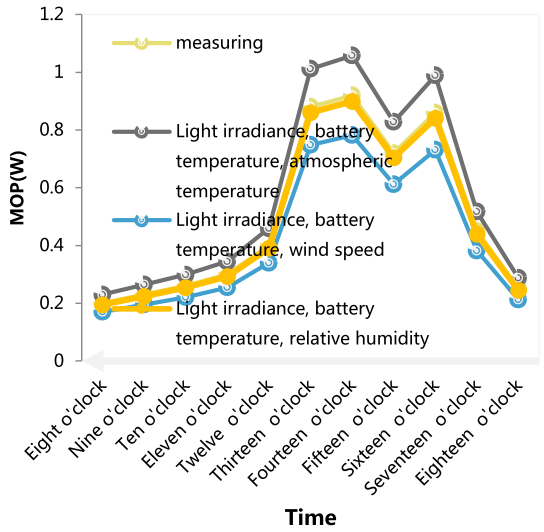

Fig. 10 Comparison of prediction results of wavelet neural network and measured values of polycrystalline silicon under various input conditions

this study studied the sum of squared error, mean square error, number of iterations, and training time of amorphous silicon under various input conditions, as shown in Table 2.

Table 2 shows that under the conditions of light irradiance, battery temperature and humidity as input, the squared error and mean square error of the network training are the smallest, and the network iterations and training time is the fastest. This shows that the power generation of amorphous silicon battery has the closest correlation with humidity, so the prediction error is small and the running speed is fast. In addition, it can be seen that relative to the prediction when light irradiance, battery temperature, and relative humidity are used as the input conditions, the network training error is large when the light irradiance, battery temperature, atmospheric temperature and when the light irradiance, battery temperature, and wind speed are used as input conditions. This shows that when the amorphous silicon battery has a weak correlation between the input amount and the predicted amount, there is a positive relationship between the training error and the speed. From the above analysis, it can be judged that the relative humidity has the strongest correlation with the maximum output power of the amorphous silicon battery, and the correlation between atmospheric temperature, wind speed and output power is weak.

Figure 10 is a comparison of the prediction results of wavelet neural network and measured values of the polycrystalline silicon under various input conditions. It can be seen from the figure that the best agreement between the predicted and measured values is still under the input conditions of light irradiance, battery temperature and atmospheric temperature. The reason is as described in the previous section. Secondly, it can be seen from the figure that the error between the predicted value and the measured value fluctuates greatly around noon (that is, between 11:00 and 14:00) when the light irradiance, battery temperature, and wind speed are input.

Figure 11 is a comparison of the prediction results of the wavelet neural network and measured values of amorphous silicon under various input conditions. It can be seen from the figure that under various conditions, the predicted value and the actual measured value generally agree well. However, the agreement is best under the conditions of light intensity, battery temperature, and humidity. However, it is the worst under the conditions of illumination, battery temperature, and atmospheric temperature, especially in the morning (9–12 pm). The reason is that the atmospheric temperature oscillations during this period are more severe, resulting in less satisfactory prediction results. The overall prediction results are consistent with the results of the previous section, that is, the predicted value and the measured value agree best under the illumination, battery temperature, and humidity conditions.

Table 2 Statistic table of sum of squared training error, mean square error, number of iterations, and training time of amorphous silicon under various input conditions

	Light irradiance, battery temperature, atmospheric temperature	Light irradiance, battery temperature, wind speed	Light irradiance, battery temperature, relative humidity
Sum of squared errors	3.153927	3.049796	2.610446
Mean square error	0.01212	0.011716	0.009999
Number of iterations	328.25	529.24	69.69
Training time	0:00:06	0:00:11	0:00:01

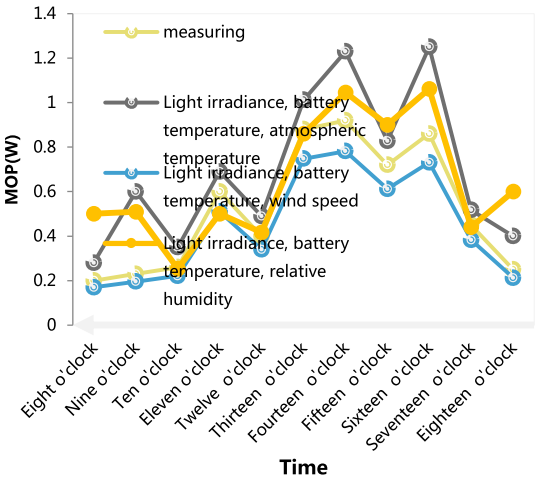

Fig. 11 Comparison of prediction results of wavelet neural network and measured values of amorphous silicon under various input conditions

The comparison between training error and prediction error of polycrystalline silicon based on BP neural network and wavelet neural network is shown in Fig. 12. From Fig. 12a–c, the SSE and MSE of the wavelet neural network trained for polycrystalline silicon can be obtained, which are much smaller than those of the BP neural network. This shows that the training of wavelet neural network is better than that of BP neural network. Moreover, the root-mean-square error RMSE value of the wavelet prediction result in Figure (c) is also smaller than the BP prediction result, which shows that the wavelet prediction is more effective than the BP prediction, that is, the prediction effect of the wavelet neural network is better than the BP neural network. From figure (c), it can also be obtained that the RMSE value predicted by the wavelet neural network or BP neural network under the conditions of illumination, battery temperature and atmospheric temperature is between 0.05 and 0.10. It shows that under these conditions, the prediction accuracy of both neural networks is high, that is, atmospheric temperature has the greatest influence on the maximum output power of photovoltaic cells.

The comparison of the training error and prediction error of amorphous silicon based on BP neural network and wavelet neural network is shown in Fig. 13. From Fig. 13a–c, it can be obtained that the SSE and MSE of the wavelet neural network training of amorphous silicon are much smaller than the values of the BP neural network. This shows that the training effect of wavelet neural network is better than the training effect of BP neural network. Moreover, the root-mean-square error RMSE value of the wavelet prediction result of figure (C) is also smaller than that of the BP prediction result. This shows that the wavelet prediction is more effective than the BP prediction, which further proves the above conclusion. In addition, from figure(c), it can be obtained that the average value of RMSE under light, battery temperature, and humidity conditions is smaller than the average value of RMSE under light, battery temperature, and atmospheric temperature and light, battery temperature, and wind speed. This shows that the relative relationship between relative humidity and amorphous silicon is the largest. The above analysis further confirms the previous analysis.

7 Conclusion

Based on artificial intelligence algorithms, this research conducted energy photovoltaic power generation forecasting. In order to determine the relationship between neural networks and external meteorological factors, a neural network prediction model and a wavelet neural network prediction model are established in this chapter. At the same time, the effects of atmospheric temperature, relative humidity, and wind speed on the power generation prediction of polysilicon cells and amorphous silicon cells were studied, and their correlations were discussed. The research is represented by the data of photovoltaic power generation in a certain area. The results show that atmospheric temperature has the strongest correlation with the output power of polysilicon cells, followed by wind speed, and finally relative humidity. Relative humidity has the strongest correlation with the output power of amorphous silicon batteries, followed by atmospheric temperature, and

Fig. 12 Comparison of training error and prediction error of polysilicon based on BP neural network and wavelet neural network

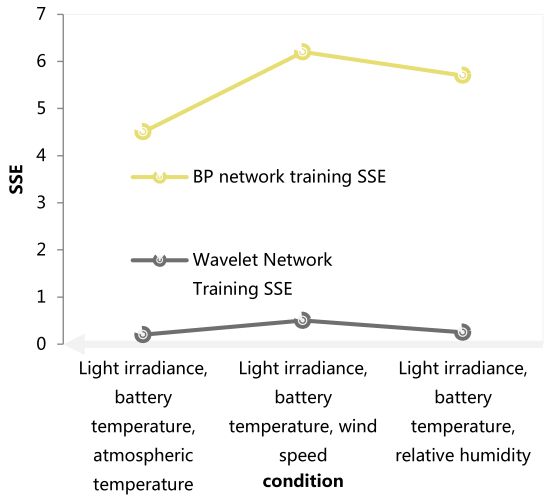

(a) SSE of BP neural network training and wavelet neural network training

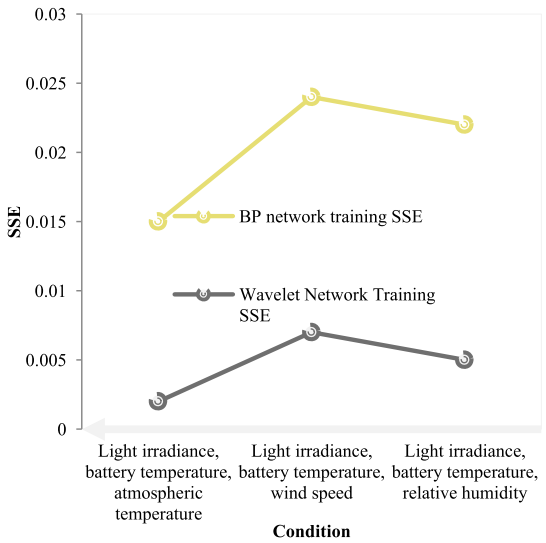

(b) MSE of BP neural network training and wavelet neural network training

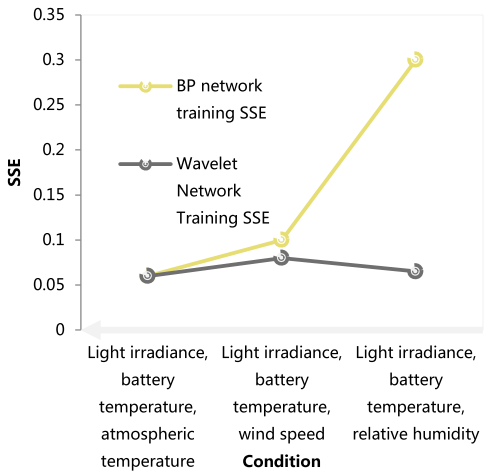

(c) Comparison diagram of root mean square error of prediction results of BP neural network and wavelet neural network

Fig. 13 Comparison of training error and prediction error of amorphous silicon based on BP neural network and wavelet neural network

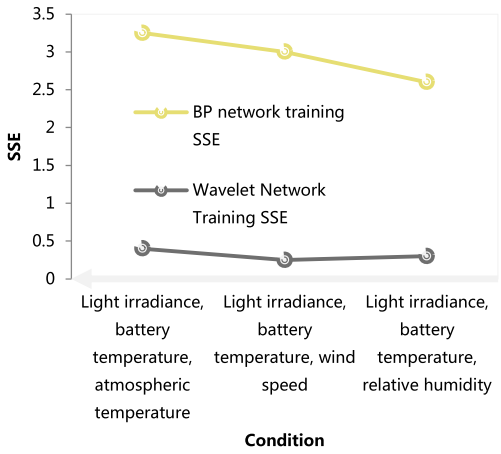

(a) SSE of BP neural network training and wavelet neural network training

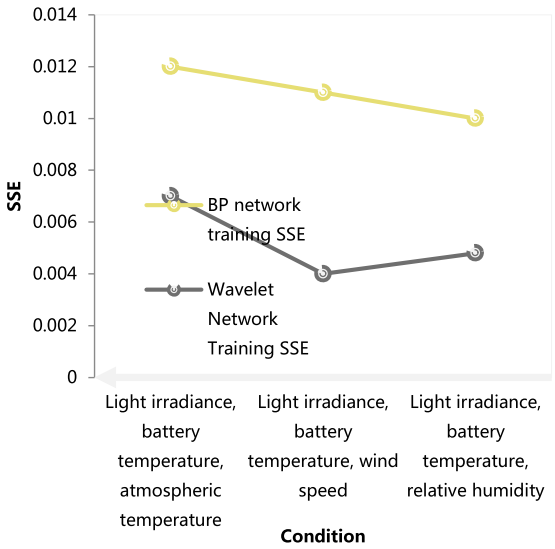

(b) MSE of BP neural network training and wavelet neural network training

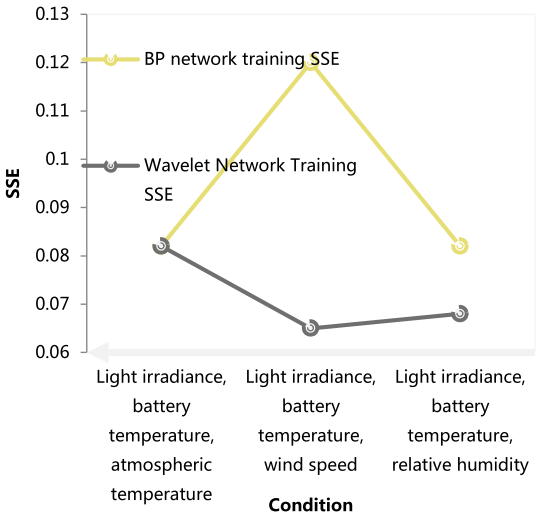

(c) Root mean square error of prediction results of BP neural network and wavelet neural network

finally wind speed. When the most relevant data is used as the input for prediction, the network training error is the smallest and the running time is the fastest. In addition, the study also found that the wavelet neural network of both silicon-based batteries is superior to the BP neural network prediction. The reason is that the wavelet function is highly adaptive and more suitable for prediction of volatility signals.

Compliance with ethical standards

Conflict of interest The authors declare that they have no conflict of interest

References

1. Cannon D, Methven J, Brayshaw DJ et al (2017) Determining the bounds of skilful forecast range for probabilistic prediction of system-wide wind power generation. Meteorol Z 26(3):239–252
2. Cheng Z, Li S, Han L et al (2017) PV power generation forecast based on data mining method. Acta Energ Solar Sin 38(3):726–733
3. Wang Z, Shen C, Liu F (2018) A conditional model of wind power forecast errors and its application in scenario generation. Appl Energy 212:771–785
4. Wu W, Wang K, Li G et al (2017) Modeling ellipsoidal uncertainty set considering conditional correlation of wind power generation. Proc Chin Soc Electr Eng 37(9):2500–2506
5. Shi Z, Liang H, Dinavahi V (2017) Direct interval forecast of uncertain wind power based on recurrent neural networks. IEEE Trans Sustain Energy 99:1
6. Jahn DE, Takle ES, Gallus WA (2017) Wind-ramp-forecast sensitivity to closure parameters in a boundary-layer parametrization scheme. Bound Layer Meteorol 164(1):475–490
7. Yatsubo O, Miyake S, Takada N (2018) Technologies for estimation and forecasting of photovoltaic generation output supporting stable operation of electric power system. IEEJ Trans Electr Electron Eng 13(3):350–355
8. Persson C, Bacher P, Shiga T et al (2017) Multi-site solar power forecasting using gradient boosted regression trees. Sol Energy 150:423–436
9. Li Q, Wu Z, Xia X (2018) Estimate and characterize PV power at demand-side hybrid system. Appl Energy 218:66–77
10. Li Q, Sun Y, Yu Y et al (2017) Short-term photovoltaic power forecasting for photovoltaic power station based on EWT-KMPMR. Trans Chin Soc Agric Eng 33(20):265–273
11. Dolatabadi A, Jadidbonab M, Mohammadi-Ivatloo B (2018) Short-term scheduling strategy for wind-based energy hub: a hybrid stochastic/IGDT approach. IEEE Trans Sustain Energy 99:1
12. Shchinnikov PA, Borush OV (2018) Results of national generation reform and predictive information about power engineering market. J Phys: Conf Ser 1111(1):012007
13. Zhang Z, Gao X, Xu T et al (2019) Electric power generation by paper materials. J Mater Chem A 7(36):20574–20578
14. Singh P, Dwivedi P (2018) Integration of new evolutionary approach with artificial neural network for solving short term load forecast problem. Appl Energy 217:537–549
15. Wang C, Zhang H, Fan W et al (2017) A new chaotic time series hybrid prediction method of wind power based on EEMD-SE and full-parameters continued fraction. Energy 138:977
16. Zhang J, Florita A, Hodge BM et al (2017) Ramp forecasting performance from improved short-term wind power forecasting. Energy 122:528–541
17. Rosenthal WS, Tartakovsky AM, Huang Z et al (2017) Ensemble Kalman Filter for dynamic state estimation of power grids stochastically driven by time-correlated mechanical input power. IEEE Trans Power Syst 99:1
18. Tian B, Piao Z, Guo D et al (2017) Wind power ultra short-term model based on improved EEMD-SE-ARMA. Power Syst Prot Control 45(4):72–79
19. Liu Y, Wang W, Ghadimi N (2017) Electricity load forecasting by an improved forecast engine for building level consumers. Energy 139:18–30
20. Wang Y, Zhang N, Chen Q et al (2019) Data-driven probabilistic net load forecasting with high penetration of behind-the-meter PV. IEEE Trans Power Syst 99:1
21. Golmohamadi H, Keypour R (2018) A bi-level robust optimization model to determine retail electricity price in presence of a significant number of invisible solar sites. Sustain Energy Grids Netw 13:93–111